Accepted Manuscript

The competition between rates of deformation and solidification in syn-kinematic granitic intrusions: Resolving the pegmatite paradox

Robert W.H. Butler, Taija Torvela

PII: S0191-8141(18)30204-9

DOI: 10.1016/j.jsg.2018.08.013

Reference: SG 3732

To appear in: *Journal of Structural Geology*

Received Date: 9 April 2018

Revised Date: 28 August 2018

Accepted Date: 28 August 2018

Please cite this article as: Butler, R.W.H., Torvela, T., The competition between rates of deformation and solidification in syn-kinematic granitic intrusions: Resolving the pegmatite paradox, *Journal of Structural Geology* (2018), doi: 10.1016/j.jsg.2018.08.013.

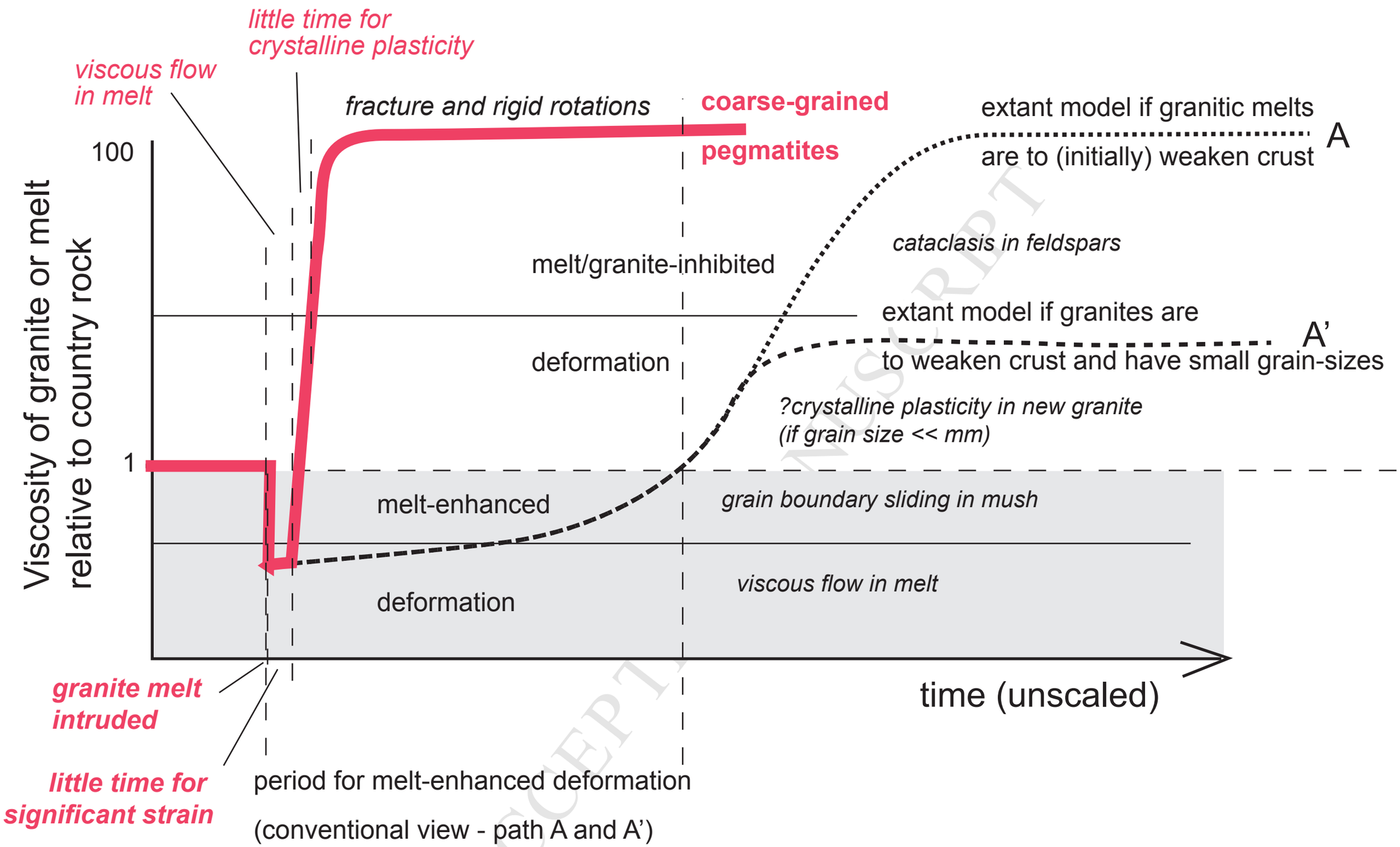

The competition between rates of deformation and solidification in syn-kinematic granitic intrusions: Resolving the pegmatite paradox

Robert W.H. Butler[a]*, Taija Torvela[b].

[a]Geology and Petroleum Geology, School of Geosciences, University of Aberdeen, Aberdeen, AB24 3UE, United Kingdom.

[b]School of Earth and Environment, University of Leeds LS2 9JT, United Kingdom

*Corresponding author: rob.butler@abdn.ac.uk

ABSTRACT

While fully-crystallized granites, rich in feldspar, generally serve to strengthen the continental crust, their precursor melts are assumed to be important agents of crustal weakening. Many syn-tectonic granitic pegmatites are deformed within shear zones but ubiquitously preserve undeformed primary magmatic textures, implying that they were largely molten during shearing. Yet the shapes of pegmatite bodies indicate that they deformed with a greater competence than their surroundings. This co-located pair of material behaviours is paradoxical. We interpret field relationships in a typical pegmatite/shear zone association (Torrisdale, NW Scotland) and propose a mechanism by which syn-tectonic granitic melts may, in effect, act as competent bodies while not yet fully crystallized. Competence was rapidly increased by preferential crystallization on intrusion margins that served to encapsulate residual melt inside stiff rinds. Further crystallization may have been pulsed as the concentrations of crystallization-inhibitors (fluxes) increased in residual fluids. Postulating the existence of initial stiff rinds also consistent with modern estimates for rates of feldspar crystallization (cms/yr) from undercooled hydrous silicic magma to form pegmatites. These greatly outpace strain-rate estimates for shear zones. Thus, fully liquid granitic melts may only be present fleetingly and have little opportunity to weaken deforming crust before crystallization begins.

Key-words: pegmatites; melt-enhanced deformation; continental deformation; rheology

1. Introduction

It is a truth universally acknowledged, that the presence of melt serves to weaken continental crust and thus strongly influence deformation (e.g., Rosenberg, 2001; Druguet and Carreras, 2006; Holzmann and Kendall, 2010). This belief arises because silicate melts have low viscosities (e.g., 10^6 – 10^8 Pa.s at 700 °C; e.g., Clemens and Petford, 1999) compared to middle crustal rocks in general (c 10^{21} – 10^{24} Pa.s: e.g. Talbot, 1999; Rybacki and Dresen, 2004). Thus, melts should weaken the bulk strength of rocks and localize deformation. This notion is exemplified by the "aneurysm" model (Zeitler et al., 2001) whereby decompression melting beneath actively eroding, deforming crust serves to focus further deformation, leading in turn to accelerated uplift, further erosion and yet more deformation. Likewise, many formulations of "channel flow", by which ductile middle crust can extrude from beneath orogenic plateaux such as Tibet, assume melt-enhanced weakening processes (e.g., Beaumont et al., 2001). The effect of melt on the pattern of deformation in contractional systems has been examined using analogue models (e.g., Zanella et al., 2014). However, for melts to have significant impact on tectonic processes, they must remain at least partially molten for time periods sufficient to accumulate significant strain. Our aim here is to examine the interplay between solidification and deformation, with specific reference to syn-tectonic granitic pegmatites.

Evidence that actively deforming continental crust once contained granitic melt include synkinematic granitic pegmatites. They are widely recorded from the exhumed parts of many different orogens (e.g. Karlstrom et al., 1993; Carreras and Druguet, 1994; Henderson and Ihlen, 2004, Selleck et al., 2005, Demartis et al., 2011), including the type area for the aneurysm model (Nanga Parbat; Butler et al., 1997). In all cases, the syn-kinematic status of the intrusions is evidenced by their cross-cut of deformation fabrics but also being deformed by folds and boudins.

A paradox lies at the heart of this truth (Fig. 1). Brown (2007, p. 417) and others argue that the crystalline granites ultimately serve to strengthen zones of crustal deformation – by adding volumes of relatively coarse-grained feldspar. Pegmatites, with their extremely coarse feldspar crystals, would be especially resistant to deformation. There are some rare exceptions, where macroscopically coarse grains have myrmekitic microstructures (e.g., Pennacchioni and Mancktelow, 2007; Pennacchioni and Zucchi, 2013), or where the pegmatites have organized networks of weak phases (e.g., quartz) that focus shearing (e.g., the 'pegmatite mylonites' of Gapais and Laouan Brer Boundi, 2014). However, the vast majority of syn-tectonic pegmatites, have two contrasting attributes: 1) they retain coarse-grained igneous textures implying that little or no internal solid-state deformation took place; and 2) the pegmatite bodies themselves display features (e.g., boudins, folds) indicative of considerable deformation. These structures imply that the pegmatite bodies were more competent than the surrounding shear zone rocks. In other words, pegmatites deform outwardly as if *more competent* than surrounding rocks, but at the same time have internal textures indicative of having been largely molten before deformation ceased and therefore, should have been *less competent* during deformation. The competing deductions, one derived from observations of internal texture, other from the shapes of the pegmatite intrusions, is the paradox to which we propose a resolution.

We examine field relationships and the internal structure of a pegmatite-shear zone system. Our field example, which displays globally typical relationships of granitic pegmatites to deformation structures, comes from the Caledonian orogen of northern Scotland. We interpret these relationships in the light of new experimental work on viscosities, solidification rates and associated crystallization sites in pegmatites. The comparison reveals that crystallization from hydrous siliceous melts, the precursors for granitic pegmatites, can be exceptionally rapid, compared to the inferred duration of deformation, but pulsed, and is probably not evenly distributed within the granitic body. All of these factors have significant consequences as to how the partially molten granitic body deforms and how it affects the bulk deformation of the crust. We will argue that neither the melts from which pegmatites crystallized, nor the

pegmatites themselves, played a significant role in weakening the crust in which they resided, thereby challenging the universal truth that magma must enhance deformation. Indeed, in the light of our observations we argue that the addition of granitic melt acts to increase the strength of shear zones, and hence, the intruded crust, even while largely liquid.

2. Assessing syn-kinematic rheology

The assumption of magma-weakening requires that melts have a lower strength than the rocks into which they intrude and that this lower strength is maintained during the deformation. Compared with more basic compositions, anhydrous siliceous melts have rather high viscosities, but they are still much weaker than the fully crystalline continental crust (e.g., Clemens and Petford, 1999). Granitic pegmatites are the crystallization products of hydrous siliceous melts. Just 2 wt % water will decrease viscosities by several orders of magnitude, compared to the anhydrous melt composition (e.g., Baker, 1998; Whittington et al., 2009; Nabelek et al., 2010). This reduction renders hydrous siliceous melts highly mobile and so they are able to migrate substantial distances rapidly from their sources, provided they retain volatiles. Hydrous siliceous melts should be very effective in focussing deformation.

The relative competence (relative variations in apparent viscosity) of components in heterogeneous rocks has long been determined from deformation structures (e.g., Ramsay, 1967; Talbot, 1999; Gardner et al., 2016). Classical diagnostic structures include pinch-and-swell structures (e.g., boudins, Fig. 2a), buckled layers (Fig. 2b), and cuspate interfaces (Fig. 2c). Boudins form in the layer with a higher competence than the surrounding material. Likewise stronger layers embedded in a weaker matrix are prone to buckling when shortened along their length (e.g., Ramsay, 1967, p. 380). Cuspate interfaces, on the other hand, are diagnostic features of ductile "flow" of the less competent material into the stronger one (e.g., Ramsay, 1967, p. 383).

More recently, studies have concentrated on the behaviour of inclusions, discrete objects either occurring individually or in trains. The relationships of inclusions to the surrounding ductile matrix foliation imply competence

contrasts (e.g., van den Dreische and Brun, 1987). Winged inclusions are particularly informative. Grasemann and Dabrowski (2015) provide results of models of competent inclusions embedded in a softer matrix undergoing simple shear, varying the viscosity contrasts and strain intensity (Fig. 2d,e). Rotation of stronger inclusions commonly results in folding of the matrix foliation at the flanks of the objects and deflection of the wings into these folds. We apply the results of Grasemann and Dabrowski (2015) to assess the relative strength of granitic melts, their crystallised products and the deforming rocks into which they were emplaced.

3. Torrisdale case study

3.1 Geological setting

Our case study comes from the exhumed middle crust of the northern Scottish Caledonides. A suite of granitic pegmatites, the Torrisdale vein complex, has intruded a dextral transpressive shear zone within the Moine thrust sheet (Holdsworth et al., 2001; Moorhouse, 2009; Strachan et al., 2010). These numerous intrusions constitute a significant percentage of the shear zone volume in this location, and are especially well-exposed in their type area at Torrisdale Bay, Sutherland (Fig. 3: 58.524N 04.254W). The pegmatites are composed of perthitic K-feldspar and albite-orthoclase with interstitial and inter-grown quartz, minor biotite and muscovite, all with cm- to dm-scale grain sizes (Holdsworth et al., 2001). The preservation of these primary crystallization textures was used to infer that the pegmatites were intruded towards the end of the regional deformation history (Holdsworth et al., 2001).

A layered sequence of locally migmatitic psammites and amphibolites form the host rocks. They contain a strong steeply- dipping, NW-SE striking foliation defined chiefly by aligned feldspar and amphiboles with mm-scale grain sizes. The prominent mineral lineation plunges moderately ESE. Garnet-pyroxene assemblages yield pre-kinematic P-T estimates of c. 650-700°C and 11-12kbar for peak metamorphic conditions but they are commonly overprinted by syn-kinematic retrograde amphibolite (Friend et al., 2000) presumably implying

deformation temperatures of 450-600°C. The migmatites yield SHRIMP U-Pb ages from zircons of 467 ±10Ma (Kinny et al., 1999). The host rock lithologies and the relationships of the host rock-pegmatite fabrics, do not provide evidence that the pegmatites were sourced locally. Consequently, their original melts migrated into their host rocks, perhaps over many kilometers.

3.2 Structure of pegmatite bodies: implications for relative competence

Typical field relationships at Torrisdale are illustrated in Fig. 4. They show that the pegmatites deformed as competent bodies. The structures are typical of syn-kinematic pegmatites that are generally interpreted to have formed after pegmatite solidification (e.g., Druguet and Carreras, 2006). The pegmatites form a variety of contorted veins up to 3-4m but commonly c. 10cm in width, together with discontinuous pods some tens of centimeters to up to several meters long. The pods are broadly parallel to the regional trend of the schistosity and lie in trains with the foliation in the surrounding rocks deflected into the necks (Fig. 4a,b). These relationships are indicative of extensive elongation of the pegmatites after their emplacement, i.e. boudinage. Other pegmatite bodies show both folds and boudins (e.g., Fig 4c,d,e). The boudins have various shapes and aspect ratios, from highly elongate (Fig. 4a,b) to short, barrel-shapes (e.g., Fig. 4, c,d,e). Although all these relationships attest to the pegmatites having greater competence than their host rocks at the time of deformation, the different forms are suggestive of a variety of competence contrasts, as implied in Fig. 2a.

Where the pegmatites are folded, the axial surfaces are sub-parallel to the foliation (Fig. 4f). Vein thicknesses are preserved around fold hinges (e.g., Fig. 4g), suggesting that they responded as single-layer buckle folds (Fig 2b: Ramsay, 1967). Therefore, as with the pegmatite pods, they had a substantially higher viscosity than the surrounding rock during deformation. Deflection of foliation around many fold hinges further attests to a high competence contrast (Fig. 4b, g). These fold trains are offset by dextral shear zones (Fig. 4e,h).

The pegmatite pods and veins commonly display cuspate margins (Fig. 4b), indicative of interfacial buckling (Fig. 2c). These relationships also imply

198 that the pegmatite body deformed with a greater competence than the
199 surrounding rocks.
200 Lastly, many pegmatite pods have flanking folds where the foliation
201 makes a high angle to the margins of the intrusions and to the regional foliation
202 trend (Fig. 4). We follow the interpretations of similar structures (e.g., Passchier
203 2001) that they form by rotation of the intrusions as bodies with viscosities
204 higher than the matrix. The foliation folds are only found adjacent to the
205 pegmatite pods, making this explanation more plausible than the proposition
206 that the pegmatites intruded fortuitously along pre-existing fold axial planes (c.f.,
207 Holdsworth et al., 2001; Moorhouse, 2010). Comparison with experiments by
208 Van den Dreische and Brun (1987) and many others since implies a strong
209 viscosity contrast between the pegmatites and matrix. Other pegmatite pods
210 have wing-like apophyses (Figs. 4i,j) that are entrained into the flanking folds
211 defined by the foliation in the country rocks. These deflections are similar to
212 those in the numerical models of Grasemann and Dabrowski (2015; Fig. 2).
213 Although the relative magnitudes of simple shear and pure shear flattening
214 across the foliation is undetermined at Torrisdale is unclear, the models of
215 Grasemann and Dabrowski (2015) indicate that shear strains in excess of 10 are
216 needed to achieve the observed geometries.
217 Bons et al. (2004) interpret trains of pod structures of pegmatites in
218 terms of elongation, arguing that they can form by differential inflation, not by
219 boudinage. However, their suggested mechanism does not explain the rotational
220 strains of the boudins recorded by deflected wall-rock foliation, the swept wing
221 shapes nor the abundant buckle folds of the associated pegmatite veins at
222 Torrisdale. All the asymmetric structures in the study area are consistent with
223 right-lateral shear, as previously reported (Strachan et al., 2010 and references
224 therein). Regardless of the kinematics, all pegmatite bodies show relationships
225 indicative of competent behaviour, with respect to the surrounding shear zone.
226 Evidence for weak behaviour, as presented by Passchier et al. (2005), is absent.
227 We therefore deduce that the pegmatites have experienced high syn-kinematic
228 strains, as opposed to having been intruded when shearing was already waning
229 (c.f. Holdsworth et al., 2001).
230

231 3.3 Internal structure of the pegmatites

232

233 The pegmatites ubiquitously show coarse textures defined principally by
234 large (5-20 cm), interlocking sub-hedral feldspar crystals. These occur together
235 with poly-crystalline quartz commonly forming irregular domains within the
236 feldspars and as intergrowths between laths (Fig. 5a, b). These are typical and
237 consistent with a primary igneous origin. They are preserved right into the necks
238 of boudins (Fig. 5f) and along folded veinlets (Fig. 5h) and are also found along
239 cuspate pegmatite interfaces (Fig. 5f). Although feldspars locally contain quartz-
240 filled fractures (Fig. 5h), these features are sparse and have very small (mm-
241 scale) offsets. Textural zoning is also common (Figs. 5c, d, e). The margins of
242 many boudins are marked by rinds of intergrown quartz and feldspar, where the
243 crystal long axes aligned sub-perpendicular to the margins of the boudins.
244 Generally these rinds are 4-6 cm wide, containing feldspar laths of about 2-6mm
245 width, locally with lengths equal to rind widths. Other rind textures include
246 patch-clusters of intergrown feldspar and quartz (Fig. 5e). The rinds pass into
247 aggregates of large feldspars (Fig. 5d).

248 The internal structure of folded pegmatite veins can also be
249 compositionally zoned. One buckled vein, 4-5 cm wide (Fig. 5g) contains a rim of
250 coarse (cm) feldspar with an interior layer of poly-crystalline quartz. Locally the
251 quartz forms elongate patches, apparently axial-planar to the folds, but without
252 alignment of individual grains. Similar quartz textures fill small fractures, in the
253 limbs and the hinge area of the folds (Fig. 5h). Elsewhere, folded pegmatite veins
254 can contain shape fabrics defined by large (5-10 mm) feldspar laths separated by
255 seams of poly-crystalline quartz with only weak grain alignment (Fig. 5i). We
256 interpret these textures to represent deformed rinds. That the feldspar crystals
257 are sub-hedral indicates that, if deformed, they achieved their orientations by
258 rigid-body rotation without any significant crystalline plasticity. The
259 polycrystalline aggregates of interstitial, sub-equant quartz presumably
260 crystallized after these deformations were achieved. Solid-state deformation, as
261 evidenced by strong shape-fabrics defined both by elongate quartz patches and
262 by individual quartz grains, is developed only very locally, at some cuspate

pegmatite boundaries (e.g., Fig. 5j), and within some wings projecting from pegmatite pods.

The observed textures imply different relationships between crystallization and deformation of the pegmatite rinds, which is illustrated schematically in Fig. 6. At low strain, fully igneous textures are preserved with feldspar laths sub-perpendicular to the intrusion walls (Fig. 6a) encased in smaller, sub-equant crystals of quartz and subordinate feldspar. However, in many examples, where interfacial buckling is recognized, and within some of the buckle-folded pegmatite veins, the feldspar laths are aligned, not perpendicular to pegmatite margins but apparently in continuity with foliation in the surrounding country rocks. Small cusps on the pegmatite margins occur between the larger feldspar laths (Fig. 6b). Yet the interstitial quartz and small sub-equant feldspar crystals between the laths have no obvious alignment. Rather they appear to have crystallized between the aligned laths. We interpret these relationships as indicative of deformation after the laths were crystallized but before the interstitial grains were crystallized. Thus, the pegmatite deformed while still retaining a melt fraction. In many cases, the texture appears to have frozen the pegmatite to resist any further internal distortion. However, at high strain locations, for example in the pinched fold hinges to some of the larger pegmatite bodies (e.g., Figs. 4c, 5j), the interstitial quartz was deformed and is now characterized by ribbon grains. (Fig. 6c) The large feldspars retain their lath shapes acquired during initial crystallization from the melt, although in some cases are fractured. Deformation must have continued after complete crystallization of the pegmatite rind.

In summary, the Torrisdale pegmatites are highly deformed, showing competent behaviour, but at the same time retain mostly undeformed magmatic internal textures. The local occurrence of rare grain-shape fabrics within deformed patches of interstitial quartz indicates that some deformation happened after solidification. However, the magmatic textures and the shapes of the pegmatite bodies themselves, was achieved before complete crystallization. Thus, competent deformation progressed during crystallization of the pegmatites. It might be expected that at least some of this deformation happened while the bodies were fully molten, with low viscosity and progressed during

296 early crystallization. Therefore, individual pegmatites should evolve from weak
297 to strong inclusions during crystallization in the deforming shear zone. Yet, no
298 weak inclusion behaviour is evident.
299
300 **4. Crystallization of pegmatites – comparisons with experiments**
301
302 Granitic pegmatites such as those found at Torrisdale are the solidification
303 products of hydrous silicic melts. They are characterised by disequilibrium
304 textures especially apparent in the relationship between quartz and feldspars,
305 such as found commonly in the Torrisdale pegmatites (Fig. 5).
306 Experimental results show the critical effects both of water and
307 undercooling on the solidification of granitic melts. Water and trace elements
308 ("fluxes") can act as crystallization inhibitors (e.g., Sirbescu et al., 2017).
309 Likewise, undercooling is the effect where material can remain fully liquid below
310 their normal liquidus, as illustrated by freezing rain, i.e., liquid water drops that
311 fall at less than 0C, freezing once they are in contact with other objects, such as a
312 road). Consider a melt at 300MPa with 5% dissolved water (e.g., Sirbescu et al.,
313 2017). It has a liquidus at c. 650°C. However, it can remain fully liquid through
314 undercooling to its glass transition, at around 350°C (e.g., Sirbescu et al., 2017).
315 The effect is to delay crystallization (e.g., London, 2011), especially where
316 experimental melts do not contain pre-existing nucleation sites to promote
317 crystallization. The consequence is that hydrous melts can retain their very low
318 viscosities, and when expelled from source migmatites they can migrate for long
319 distances before being emplaced into cooler rocks. Presumably the principal
320 migration path away from the source migmatites is along fracture systems (e.g.,
321 Brown, 2007).
322 Once it begins, crystallization from strongly undercooled hydrous melts is
323 exceptionally fast (e.g., Webber et al., 1999). Baker and Freda (2001) report
324 feldspar crystal growth rates from experiments of up to $5x10^{-9}m.s^{-1}$. Therefore,
325 10cm feldspar crystals, such as those found in the Torrisdale pegmatites, could
326 grow in a few years or less. Furthermore, as undercooling inhibits nucleation,
327 few very large crystals grow exceptionally rapidly (e.g., Nabelek et al., 2010).
328 This will have the effect of creating aggregates of very coarse, sub-hedral

feldspar crystals within melt-pods. We suggest that the rigid-body interactions of these new large crystals will significantly increase the strength of the pods, even with significant volumes of melt remaining. If the host rock of the intrusions has comparatively small grain size, or significant proportions of weak phases (e.g., mica), this process could result in a competence contrast where the partly crystallized body has a higher competence than the finer-grained host rock.

Recent experimental results by Sirbescu et al. (2017) extend the earlier results with rates of $2.5x10^{-9}m.s^{-1}$ for crystallization of a granitic melt with 6.5% wt% H_2O at 500 °C. Critically, they show that the growth of blades of feldspar, by unidirectional crystallization, can occur through nucleation on the wall of the experimental vessel (Figs. 6d, e), and are largely absent from the experimental melt interior. We equate these virgilite grain textures in the experiments to be geometrically equivalent to feldspar grain textures in the pegmatites at their boundaries (Figs. 6a, b, c). Given the geometric equivalency, we infer that the feldspars had similar crystallization histories to the virgilite, so that the Torrisdale rinds could form in about one year, encapsulating residual melt that subsequently crystallized as larger feldspar crystals.

Preferential crystallization of large feldspars on intrusion walls creates an armoured rind so that the interface of the intrusion is stronger than the surrounding shear zone, even if the rind encapsulates much weaker residual liquid. Contraction of the interface could pack the rind-forming feldspar laths more closely (Fig. 6b). While these laths may experience rigid rotation and grain-boundary sliding, any interstitial quartz may deform plastically (Fig. 6c). A similar behaviour may occur in the buckled veins. Rigid rotation or grain-boundary sliding of feldspar laths can define preferred orientations and the weak fanning around the folds, while the quartz, if crystallized, can deform plastically. If residual melt remains it may also be redistributed to other sites in the vein through tectonic compaction.

Continued deformation acting on the pods of residual melt could cause rupture of the encapsulating rinds. The wings to rotated inclusions, and the long veinlets found at Torrisdale may reflect this process. However, these redistributive processes require complex, pulsed crystallization histories. The experiments of Sirbescu et al. (2017) do indeed show complex, non-steady

crystallization behaviours and textures that mimic the complexity of natural pegmatites. They include the partial reabsorption of phases, replacive textures and zoned growth. This behaviour and resultant textures appear to be in response to small variations in the concentrations of exsolved water and the residual crystallization inhibitors ("fluxes") in the remaining liquid. Deformation could act as a further forcing agent away from steady-state crystallization, especially through rind-rupture. This could lead to significant draining from the pods, with pressure reductions and reorganization of local heterogeneities in the residual liquid. The complexity of textures seen in syn-kinematic pegmatites is therefore to be expected, when related to the complex crystallization behaviours in these experiments.

5. Implications for deformation – competing rates

Two basic tenets underlie the consideration of granitic melts: their solidification and the effect of their rheology relative to that of a surrounding shear zone. First, partial melts are always weaker than their fully solid hosts and that the magnitude of strength drop is controlled principally by the relative proportion of solid crystal vs. melt, known as the melt fraction (e.g., Arzi, 1978; and many others since). Second, crystallization is considered to occur very close to the liquidus of the melt and that this happens in relatively slow and steady over time. Therefore, melt is present for long durations and consequently is available to influence deformation for extended periods of time (e.g., Davidson et al., 1994).

The growth of crystals floating within residual melt may conform to rheological descriptions modified from Arzi's (1978) critical melt fraction and derivations thereafter. However, we suggest that where crystals interact with the melt margins, and especially if crystallization forms rinds, these prior concepts are insufficient for the circumstances described here. The experimental results of Sirbescu et al (2017) show the importance of nucleation sites in the solidification history of undercooled hydrous granitic melts. Therefore, when considering the rheological behaviour of these systems in terms of simple crystal-residual liquid mixtures, perhaps a better geometric description is a viscous liquid encased in a

competent rind. Small amounts of fractional crystallization, focussed on intrusion margins, could increase the effective viscosity of the entire intrusion and exceed that of the surrounding rocks, especially if those country rocks are relatively fine-grained. Granites will only weaken shear zones for as long as they have lower effective viscosities than their surroundings. If crystallization starts as the melt is emplaced, and is as rapid as measured in the experiments, the presence of weak material is fleeting.

We can contrast the behaviour deduced for the Torrisdale setting with a conventional view of magma-enhanced weakening in shear zones developed in continental crust (except for those in restitic dry granulites from which fluxes have been extracted; c.f., Menegon et al., 2011). Figure 7 is a qualitative illustration of the syn-kinematic evolution of the viscosity contrast between wet granite and deforming country rocks during crystallization within a deforming crustal volume. As Brown (2007) and others note, the fully crystallized granitic bodies are stronger than the surrounding shear zone rocks because of their higher feldspar content and their greater grain sizes. To reach a fully crystallized state, a siliceous melt evolves from completely liquid, through a partially-crystallized state, commonly viewed as a 'crystal mush' (e.g., Arzi 1978). For the conventional model of slow crystallization from crystal mush (paths A and A', depending on final grain size, Fig. 7), an extended period of time exists where the melt remains relatively evenly distributed and in considerable proportion, with gradual crystallization. Thus, the viscosity will increase gradually, following a pattern predicted from the temperature-dependent viscosity of residual liquid and the proportion of crystallized solid phases, where the main melt-fraction threshold for significant strength change is estimated at only a few percent (e.g., Rosenberg and Handy, 2005). Complexities in the rheology of these systems are discussed by Vigneresse (2015). The final viscosity of the resultant fully crystalline granite will, for a given temperature, strain rate and composition, be largely controlled by its grain size (compare A with A' on Fig. 7). Therefore, coarse-grained granitic pegmatites are expected to be stronger than an equivalent granite with smaller grain sizes, but both are expected to deform internally while they were still partially molten.

Contrast the conventional histories, represented by paths A and A', with the scenarios proposed for pegmatites such as those we have described from Torrisdale (path B on Fig. 7). Note that there is only one outcome (B) on Fig. 7 because, by definition, pegmatites are always coarse-grained. Crystallization initiates rapidly upon emplacement and is concentrated on the margins of the intrusions. Further, the bulk strength of the intrusion is not a direct function of melt fraction but is dependent on the formation of the stiff rinds and their resultant thicknesses. We propose that these intrusions rapidly become stronger than their surroundings even though they may be retain significant residual melt because of their rinds. Full crystallization subsequent to the initial rapid crystallization of the rinds may be protracted, but the intrusions ubiquitously behave as inclusions with viscosities greater than the surrounding shear zone.

How much deformation might be achieved in the fleetingly short period before significant rinds have crystallized on intrusion walls? The answer to this question depends on the strain rate and the available time for deformation while feldspars are sufficiently fine-grained to accommodate significant strain by crystal-plasticity. Viegas et al. (2016) suggest high strain rates are possible for deformation acting on fine aggregates of previously cataclased feldspars, but these textures are absent at Torrisdale. In the following thought experiment, we develop two arguments for strain rate, where one is derived from microstructure and the other is developed from consideration of time-averaged fault-slip rates.

Microstructurally-constrained strain-rate estimates for feldspathic rocks are highly variable but, for temperatures of deformation of 450-500°C ,the fastest values do not exceed about 10^{-12} s^{-1} (e.g., Rybacki and Dresen, 2004), even for diffusion creep and fine grain sizes (<50 μm). So, we adopt this value as the fastest possible strain rate that the pegmatites must accommodate if they were to enhance deformation in the shear zone. Alternatively, we can consider the shear zone that hosts the pegmatites at Torrisdale coupled directly with a typical continental fault zone. If the active shear zone has a width of between 1 km and 100 m, and accommodated slip on the fault an exceptionally rapid rate of about 3 cm/yr, the resolved strain rate is 10^{-11} – 10^{-12} s^{-1}. Both arguments thus yield peak strain rates of c 10^{-12} s^{-1}. So, how much deformation can accumulate in the time while feldspars in the fledgling pegmatite rinds are still fine-grained? We

conservatively estimate this available time to be one year, based on the experimental results of Sirbescu et al. (2017). The amount of shear strain that the shear zone could accommodate in this time is vanishingly small ($<10^{-2}$). In contrast, a possible shear strain of 10, implied by boudin rotations, would take minimum of thousands of years to accumulate. Therefore, we conclude that any weakening in the shear zone caused by the emplacement of the initial melt would be so transient as to lack tectonic significance.

6. Structurally-controlled fractional crystallization?

If rapid crystallization continues under relatively slow strain rates, pegmatites will 'freeze' and either cease deforming or deform plastically during subsequent strain. For the pegmatite bodies to retain igneous textures while still deforming as rigid bodies, enabled by the crystalline rinds, full crystallization must have been retarded after initial rapid growth. Nabelek et al. (2010) argue that zoned pegmatites, such as seen in Fig. 4, may reflect interrupted crystallization caused by a build up in the residual liquid of water and other fluxes. Given that crystallization does not simply relate to cooling and its time-line is not necessarily linear (e.g., London, 2014), fractional crystallization can be pulsed, with periods of rapid growth, perhaps modulated and retarded by, for example, the latent heat of crystallization in adjacent grains (e.g., Sirbescu et al., 2008). In these deforming partial melts, the residual fluids may be expelled into secondary veins when rinds locally rupture, or be trapped in interstitial sites within the stiff crystal framework. Although even small percentages of melts in a rock volume theoretically weaken the bulk rock (e.g., Rosenberg and Handy, 2005), the coarse-grained feldspars interlock, giving even the partly crystallized pegmatite greater strength than the finer-grained, less feldspathic host rocks. Deformation within these partly-crystallized but competently-behaving bodies could occur by grain-boundary sliding (granular flow), accommodating the folding and the boudinage but without producing crystal-plastic deformation fabrics within the pegmatite (see also Rosenberg and Berger, 2001).

As crystallization progresses in a pegmatite, the residual melt will become increasingly enriched in incompatible elements, some of which can continue to

act as fluxes, further inhibiting crystallization and suppressing viscosity. This low-viscosity melt would be encapsulated within a crystallized rind and as interstitial liquid between large, rigid feldspar laths. Thus, the composite material, namely the solidifying pegmatite, is stronger than the surrounding shear zone rocks. However, ruptures of the rind could allow stringers of melt escape, forming winged intrusions. The loss of flux-rich liquid and the local pressure-drop within the ruptured capsule (future pegmatite pod) may in turn promote crystallization for the residual fluid (e.g., Webber et al., 1999). Fully crystallized pegmatites can therefore be compositionally, and texturally zoned. This model provides explanations for the complexity of textures and structure in deformed pegmatites. However, many existing studies of these processes consider undeformed pegmatite arrays (e.g., Webber et al., 1999). When emplaced into active shear zones, such as in our example from Torrisdale, the structural evolution may strongly influence fractional crystallization. It may be tested through carefully mapping the relationship between stringers, larger pegmatite bodies that source them and their internal textures, using these geometric relationships to erect a relative history of crystallization, deformation and rind-rupture. Later crystallized phases should be increasingly enriched in incompatible elements, if the studied system is closed. However, given the large grain-sizes and potentially complex zonal growth patterns, such linked structure/microstructural and microchemical analysis would not be simple.

7. Tectonic implications

The role of undercooled hydrated granitic melts, the forerunners to pegmatites, in weakening actively deforming crust may be over-estimated. Initial crystallization, preferentially located on intrusion walls can occur over time-periods that are too short (< a year) to accumulate significant tectonic strain. Likewise, estimated melt-fractions need not be a guide to bulk strength of solidifying pegmatites if initial crystallization forms rinds. Melts do not have to completely solidify before deformation to deform competently. Furthermore, as very little or no ductile deformation in Torrisdale is observed after folding, boudinage, and the subsequent complete solidification of the pegmatites, the

process of syn-crystallization deformation served to increase the strength of this portion of crust, resulting in the deformation moving elsewhere.

Granitic pegmatites, similar in structure to those we describe from Torrisdale, are the principal syn-tectonic magmatic rocks at Nanga Parbat (NW Himalyas) where they underpin the notion that decompression melting has enhanced crustal-scale deformation (the aneurysm model of Zeitler et al., 2001. But, as noted elsewhere (Butler, in press), melting and the emplacement of undercooled granitic melts may act to inhibit rather than promote deformation.

We concur with others (e.g., Neves et al., 1996; Brown, 2007) that fully crystallized granites strengthen the continental crust. However, previous work (e.g., Druguet and Carreras, 2006) suggests that such competence reversal happens after crystallization of melts, not during. We suggest that rapid initial crystallization results in stiff rinds and coarse interlocked grains; this combined with encapsulation of residual fluids allows pegmatites to deform as stiff partial melts. The rate of crystallization, coupled with crystallization sites, relative to strain rate is key. Further work is now needed to explore the rheological impacts of the causes and the relationships between the rates of crystallization, strain rates, grain size of (partly) crystallized melts vs. host rocks, and deformation in various tectono-magmatic systems, together with how deformation can influence the sites of fractional crystallization and the fate of residual fluids and fluxes in these systems. Indeed, recent work by Lee et al. (2018) suggests that 'freezing' of partial melts within migmatitic, non-pegmatite-bearing syn-melt shear zones also occurs. The 'melt-strengthening' behaviour may be more common and more important to the behaviour of orogenic crust than previously realized. This has potentially profound implications: the crystallization rate is critical to whether presence of melts weaken or strengthen the orogenic crust.

8. Conclusions

That granite pegmatites deform as if more competent than their surroundings, yet internally preserve ubiquitous igneous textures, is an apparent paradox. We resolve this conundrum by interpreting field observations in the light of published results from solidification experiments on undercooled hydrous

559 granitic melt (Sirbescu et al., 2017). These experiments show that crystallization
560 is inhibited but once it begins, can be initially exceptionally fast (cm/yr). The
561 initial crystallization rates greatly outpace natural strain rates in shear zones. In
562 many pegmatites, the first crystals form preferentially on intrusion margins.
563 Natural textures in the studied pegmatites include coarse-grained feldspar-rich
564 rinds that we interpret as having encapsulated residual melts. Solidification may
565 have been pulsed as the residual melt became enriched in incompatible elements
566 that acted as crystallization inhibitors (chemical fluxes). Thus, significant melt
567 can remain during deformation, but these partially-solid pegmatite bodies can be
568 stronger than the shear zones within which they are emplaced. Our case study
569 from Torrisdale (NW Scotland) displays field relationships that are common to
570 pegmatite-bearing shear zones elsewhere (Karlstrom et al., 1993; Henderson
571 and Ihlen, 2004), and so we propose that the following deductions apply
572 generally to these systems. First, the lack of recognised weak-inclusion
573 behaviour imply that the pegmatites accommodated no significant strain while
574 retaining viscosities of fully liquid, hydrous siliceous melts. Second, we suggest
575 that: i) melt distribution is more important than melt fraction for the rheological
576 behaviour of partial melts; and ii) the incompetence of partial melt bodies is only
577 fleeting, as the emplaced granitic magma does not get the opportunity to
578 accumulate significant strain. These partial melts will not therefore have
579 provided a significant weakening mechanism in shear zones, and indeed, they
580 represent an addition of competent material.
581
582 Acknowledgements.
583 We thank Ian Alsop and Rob Strachan for discussions on the deformation at
584 Torrisdale together with Alan Whittington and Mona-Liza Sirbescu for
585 discussions and sharing manuscripts on melt rheologies and pegmatite
586 crystallization. We also thank Elena Druguet for comments on a draft of these
587 ideas, Luca Menegon and Denis Gapais for vigorous reviews of this paper, Bill
588 Dunne for his editorial sweep-through, and participants at DRT2017 in Inverness
589 for comments, in and out of the field. However, the views expressed here are
590 exclusively those of the authors.
591

592 **References**

593

594 Arzi, A.A., 1978. Critical phenomena in the rheology of partially melted rocks.
595 Tectonophysics 44, 173-184.
596 Baker, D.R., 1998. Granitic melt viscosity and dike formation. Journal of
597 Structural Geology 20, 1395-1404.
598 Baker, D.R., Freda, C., 2001. Eutectic crystallization in the undercooled
599 orthoclase-quartz-H2O system: experiments and simulations. European
600 Journal of Mineralogy 13, 453-466.
601 Beaumont, C., Jamieson, R.A., Nguyen, M.H., Lee, B., 2001. Himalayan tectonics
602 explained by extrusion of a low-viscosity crustal channel coupled to focused
603 surface denudation. Nature 414, 738–742.
604 Bons, P.D., Druguet, E., Hamann, I., Carreras, J., Passchier, C.W., 2004. Apparent
605 boudinage in dykes. Journal of Structural Geology 26, 625-636.
606 Brown, M., 2007. Crustal melting and melt extraction, ascent and emplacement in
607 orogens: mechanisms and consequences. Journal of the Geological Society,
608 London 164, 709-730.
609 Butler, R.W.H. (in press). Structural evolution of the Himalayan syntaxes: the
610 view from Nanga Parbat. In Treloar, P., Searle, M. (Eds.) Himalayan tectonics: a
611 modern synthesis. Geological Society, London Special Publications, 483,
612 Butler, R.W.H., Harris, N.B.W., Whittington, A.G., 1997. Interactions between
613 deformation, magmatism and hydrothermal activity during active crustal
614 thickening: a field example from Nanga Parbat, Pakistan Himalayas.
615 Mineralogical Magazine 61, 37-52.
616 Carreras, J., Druguet, E., 1994. Structural zonation as a result of inhomogeneous
617 noncoaxial deformation and its control on syntectonic intrusions: an
618 example from the Cap de Creus area (eastern-Pyrenees). Journal of
619 Structural Geology 16, 1525-1534.
620 Clemens, J.D., Petford, N. 1999. Granitic melt viscosity and silicic magma
621 dynamics in contrasting tectonic settings. Journal of the Geological Society,
622 London 156, 1057-1060.
623 Davidson, C., Schmid, S.M., Hollister, L.S., 1994. Role of melt during deformation
624 in the deep crust. Terra Nova 6, 133–142.

625 Demartis, M., Pinotti, L.P., Coniglio, J.E., D'Eramo, F.J., Tubia, J.M., Insua, L.A.A.,
626 2011. Ascent and emplacement of pegmatite melts in a major reverse shear
627 zone (Sierras de Cordoba, Argentina). Journal of Structural Geology 33, 1334-
628 1346.
629 Druguet, E., Carreras, J., 2006. Analogue modelling of syntectonic leucosomes in
630 migmatitic schists. Journal of Structural Geology 28, 1734-1747.
631 Friend, C.R.L., Jones, K.A., Burns, I.M., 2000. New high-pressure granulite facies
632 event in the Moine Supergroup, northern Scotland: implications for Taconic
633 (early Caledonian) crustal evolution. Geology 28, 543-546.
634 Gardner, R.L., Piazolo, S., Daczko, N.R., 2016. Shape of pinch and swell structures
635 as a viscosity indicator: Application to lower crustal polyphase rocks. Journal
636 of Structural Geology 88, 32-45.
637 Grasemann, B., Dabrowski, M., 2015. Winged inclusions: Pinch-and-swell objects
638 during high-strain simple shear. Journal of Structural Geology 70, 78-94.
639 Henderson, I.H.C., Ihlen, P.M., 2004. Emplacement of polygeneration pegmatites
640 in relation to Sveco-Norwegian contractional tectonics: examples from
641 southern Norway. Precambrian Research 133, 207-222.
642 Holdsworth, R.E., Strachan, R.A., Alsop, G.I., 2001. Solid geology of the Tongue
643 district. Memoir for 1:50,000 geological sheet 114E. British Geological Survey,
644 London, pp.75.
645 Holtzman, B.K., Kendall, J.M., 2010. Organized melt, seismic anisotropy, and plate
646 boundary lubrication. Geochemistry Geophysics Geosystems 11,
647 doi:10.1029/2010GC003296.
648 Karlstrom, K.E., Miller, C.F., Kingsbury, J.A., Wooden, J.L., 1993. Pluton
649 emplacement along an active ductile thrust zone, Piute Mountains,
650 southeastern California: Interaction between deformational and solidification
651 processes. Geological Society of America Bulletin 105, 213–230.
652 Kinny, P.D., Friend, C.R.L., Strachan, R.A., Watt, G.R., Burns, I.M., 1999. U-Pb
653 geochronology of regional migmatites in East Sutherland, Scotland: evidence
654 for crustal melting during the Caledonian orogeny. Journal of the Geological
655 Society, London 156, 1143-1152.
656 Lee, A.L., Torvela, T., Lloyd, G.E., Walker, A., 2018. Melt organization and strain
657 partitioning in the lower crust. Journal of Structural Geology 113, 188-199.

London, D., 2011. Experimental synthesis and stability of tourmaline: A historical overview. Canadian Mineralogist 49, 117–136.

London, D., 2014. Subsolidus isothermal fractional crystallization. American Mineralogist 99, 543-546.

Moorhouse, V.E., 2009. Aird Torrisdale. In Mendum, J.R., Barber, A.J., Butler, R.W.H., Flinn, D., Goodenough, K.M., Krabbendam, M., Park, R.G. Stewart, A.D. (Eds.) Lewisian, Torridonian and Moine Rocks of Scotland. Geological Conservation Review Series 34, Joint Nature Conservation Council, Peterborough, 404-410.

Nabelek, P.I., Whittington, A.G., Sirbescu, M-L. C., 2010. The role of H_20 in rapid emplacement and crystallization of granite pegmatites: resolving the paradox of large crystals in highly undercooled melts: Contributions to Mineralogy and Petrology 160, 313-325.

Neves, S.P., Vauchez, A., Archanjo, C.J., 1996. Shear zone-controlled magma emplacement or magma-assisted nucleation of shear zones? Insights from northeast Brazil. Tectonophysics 262, 349-364.

Passchier, C.W., 2001. Flanking structures. Journal of Structural Geology 23, 951-962.

Passchier, C.W., Mancktelow, N.S., Grasemann, B., 2005. Flow pertubations: a tool to study and characterise heterogeneous deformation. Journal of Structural Geology 27, 1011-1026.

Ramsay, J.G., 1967. Folding and fracturing of rocks. McGraw Hill, New York, pp. 568.

Rosenberg, C., 2001. Deformation of partly molten granite: a review and comparison of experimental and natural case studies. International Journal of Earth Sciences 90, 60-76.

Rosenberg, C.L., Handy, M.R., 2005. Experimental deformation of partially melted granite revisited: Implications for the continental crust: Journal of Metamorphic Geology 23, 19–28.

Rybacki, E., and Dresen, G., 2004. Deformation mechanism maps for feldspar. Tectonophysics 382, 173-187.

Selleck, B.W., McClelland, J.M., Bickford, M.E., 2005. Granite emplacement during tectonic exhumation: The Adirondack example. Geology 33, 781-784.

691 Sirbescu, M-L., Hartwick, E.E., Student, J.J.,2008. Rapid crystallization of the
692 Animikie Red Ace Pegmatite, Florence County, northeastern Wisconsin:
693 inclusion microthermomettry and conductive-cooling modelling.
694 Contributions to Mineraology and Petrology 156, 289-305.
695 Sirbescu, M-L. Schmidt, C., Velsler, I.V., Whittington, A,G., Wilke, M., 2017.
696 Experimental Crystallization of Undercooled Felsic Liquids: Generation of
697 Pegmatitic Texture. Journal of Petrology 58, 539–568.
698 Strachan, R.A., Holdsworth, R.E., Friend, C., Burns, I., Alsop, I., 2010, North
699 Sutherland. In Strachan, R., Alsop, I., Friend, C., Miller, S. (Eds.) An excursion
700 guide to the Moine geology of the northern Highlands of Scotland. National
701 Museums of Scotland, Edinburgh, 231-265.
702 Talbot, C.J., 1999. Can field data constrain rock viscosities? Journal of Structural
703 Geology 21, 949-957.
704 Van den Driessche, J., Brun, J-P., 1987. Rolling structures at large shear strains.
705 Journal of Structural Geology 9, 691-704.
706 Vigneresse, J-L., 2015. Textures and melt-crystal-gas interactions in granites.
707 Geoscience Frontiers 6, 635-663.
708 Webber, K.L., Simmons, W.B., Falster, A.U., Foord, E.E., 1999. Cooling rates and
709 crystallization dynamics of shallow level pegmatite-aplite dikes, San Diego
710 County, California. American Mineralogist 84, 708-717.
711 Whittington, A.G., Bouhifd, M.A., Richet., P., 2009. The viscosity of hydrous
712 $NaAlSi_3O_8$ and granitic melts: configurational entropy models. American
713 Mineralogist 94, 1–16.
714 Zanella, A., Cobbold, P.R., Le Carlier de Veslud, C., 2014. Physical modeling of
715 chemical compaction, overpressure development, hydraulic fracturing and
716 thrust detachments in organic-rich source rock. Marine and Petroleum
717 Geology 55, 262-274.
718 Zeitler, P.K., Meltzer, A.M., Koons, P.O., Craw, D., Hallet, B., Chamberlain, C.P.,
719 Kidd, W.S.F., Park, S., Seeber, L., Bishop, M., Shroder, J., 2001. Erosion,
720 Himalayan geodynamics and the geomorphology of metamorphism. GSA
721 Today 11 (1), 4–9.
722
723

724

Figure captions

Figure 1. The pegmatite paradox. Intrusions preserve igneous textures indicative of no significant internal (solid-state) deformation, yet have external shapes indicative of having deformed but with a greater competence than their surroundings. If the intrusions deformed while still largely molten - as implied by their internal texture - why do they not show weak (less competent) inclusion behaviour?

Figure 2. Assessing relative competence in heterogeneously deformed rocks. Classic approaches are shown in a-c, after Ramsay (1967). a) evolving boudinage, where four layers are shown with increasing competence (1 to 4) and the matrix has the same competence as layer 1. b) single-layer buckle folding, with layers of increasing competence (1-5), the matrix competence equals layer 1. c) interfacial buckling. d) and e) show results from numerical modelling by Grasemann and Dabrowski (2015), for winged inclusions with competence contrasts (v) relative to matrix and initial aspect ratios of 3:1 (d) and 2:1 (e). Deformation is homogeneous right-lateral simple shear with shear strains of 10 (left) and 20 (right).

Figure 3. Simplified geological map for the Torrisdale Bay study area (after Moorhouse, 2010). The grid is UK National Grid (sector NC). Inset: N Scotland location map.

Figure 4. Detailed outcrop sketch maps and photographs showing the shapes of pegmatite intrusions and their relationships to the principal deformation foliation in the surrounding rocks. These outcrops all lie within a 150m square area centred on grid reference NC 688616. In all sketches, the pegmatites are grey and do not show internal foliations. The half-arrows show dextral shear, inferred from structures within the outcrops and the deflections of flanking folds at pegmatite bodies. Various details are shown in Fig. 5. a) Typical pod-form of the pegmatites, with flanking folds and apophyses. The boxed areas x and y are details shown in Fig. 5 d and f respectively. b) panoramic photograph of (Fig. 4a);

c) Folded and boudinaged pegmatite sheet. X is labelled to tie to photographs; d) oblique photograph looking SSW along the outcrop in Fig. 4c (refer to this for scale); e) oblique photograph looking NNE. f) train of pegmatite pods with pegmatite stringers that form deformed apophyses from the pods. The pods are identified (S-V). The folded stringer is interpreted to be a single original vein so that labelled elements X, Y and Z were once continuous but have been separated by right-lateral shear. The boxed area locates Fig. 4g and is c 30 cm long. g) oblique photograph showing detail of folded single layer of pegmatite. h) a general oblique photograph of the outcrop sketched on Fig. 4f. The labelled sites tie to Fig. 4f which also gives the scale. i) part of a string of pegmatite pods which, in common with many others, preserve igneous textures right into the thin necks. The pods have flattened apophyses that are deflected into the surrounding foliation which locally displays flanking folds against pegmatite pods. j) oblique photograph of the pegmatite pods shown in Fig. 4i (refer to this for scale).

Figure 5. Details of the internal texture of the pegmatites and their interpretation as records of progressive deformation during crystallization. These outcrops all lie within grid reference NC 688616. a) wide-shot of a pegmatite pod with flanking folds. The pen is 15 cm long. b) detail (boxed area on a) showing very coarse primary feldspar crystals with irregular clusters of polycrystalline quartz. These textures are preserved throughout the pod. The coin is 2 cm in diameter. c) typical margin facies showing laths of feldspar that grew sub-perpendicular to the pegmatite wall. The laths are separated by domains of polycrystalline quartz. The coin is 2 cm in diameter. d) detail of pegmatite margin (boxed area x on Fig. 4a). The coin is 2 cm in diameter. e) coarse margin facies in pegmatite (just right of x on Fig. 4a). The coin is 2.8 cm in diameter. f) detail of the boudin tail (y on Fig. 4a) showing retention of igneous texture with coarse feldspar regardless of the thickness of the pegmatite and the intensity of its necking. The coin is 2.8 cm in diameter. g) folded stringer of pegmatite (boxed area of Fig. 4g). The coin is 2.2 cm in diameter. h) detail of fold hinge (boxed area in Fig. 5g) showing fanning fabric of feldspar laths enclosing linear domains of polycrystalline quartz. The coin is 2.2 cm in diameter. i) deformed igneous textures in hinge of a folded

pegmatite stringer with cuspate interface indicative of pegmatite having deformed with a greater competence than its wall rocks. The coin is 2.2 cm in diameter. j) detail of a hinge in folded pegmatite showing different size-orders of interfacial buckling. The coin is 2.8 cm in diameter.

Figure 6. Illustrations of textures on the margins of the pegmatites, their relationship to deformation and comparisons with experimental textures reported by Sirbescu et al. (2017). Note common scale bar for a-c. a) large, aligned feldspar crystals at a margin for low deformation state. b) a similar marginal facies but inferred to have deformed while crystallizing so that the large feldspars are rotated with the intrusion wall but interstitial crystals are not. c) deformation of the marginal rind after complete crystallization, with interstitial quartz forming ribbon grains indicative of sold-state crystal-plasticity. The experimental textures (d,e) show preferential crystallization on the wall of the vessel, with residual melt quenched to form glass. d) virgilite (lithium aluminium silicate) grown on walls after 5 days, at 500 °C and 300 MPa. The apparently floating crystals are inferred connect to the rim out of the plane of section. e) skeletal alkali feldspar and clusters of intergrown albite, orthoclase and quartz. The experiment ran for 9 days at 600 °C and 300 MPa.

Figure 7. Qualitative representation of the evolution of viscosity of siliceous melt crystallizing into granite through time that contrasts a conventional view of granite behaviour (A, A') with that deduced here for the pegmatites (B). Note that melt-enhanced deformation happens when the relative viscosity is less than 1. The duration of this low-viscosity behaviour governs the amount of deformation that could be melt-enhanced for a given strain rate.

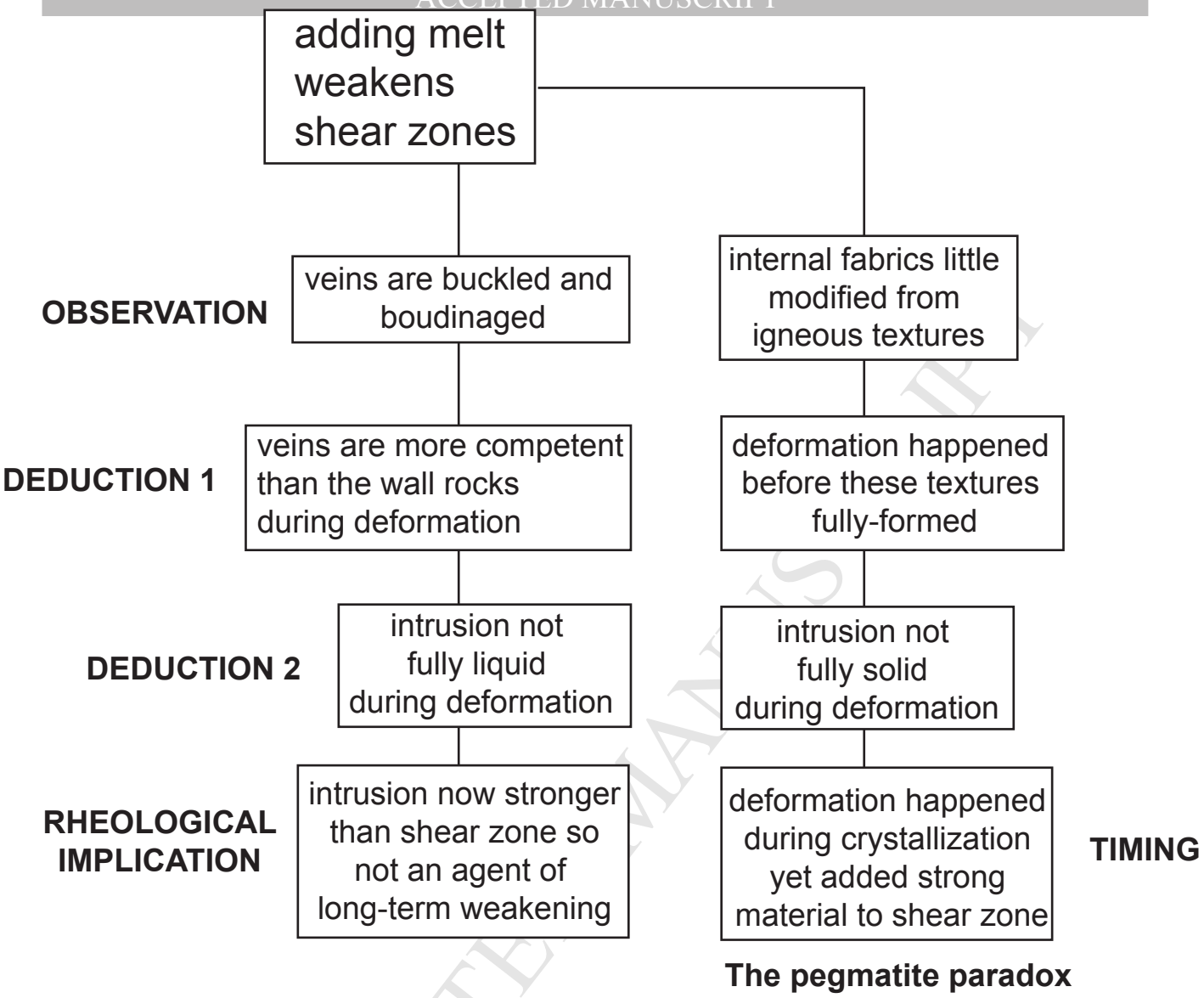

Fig 2

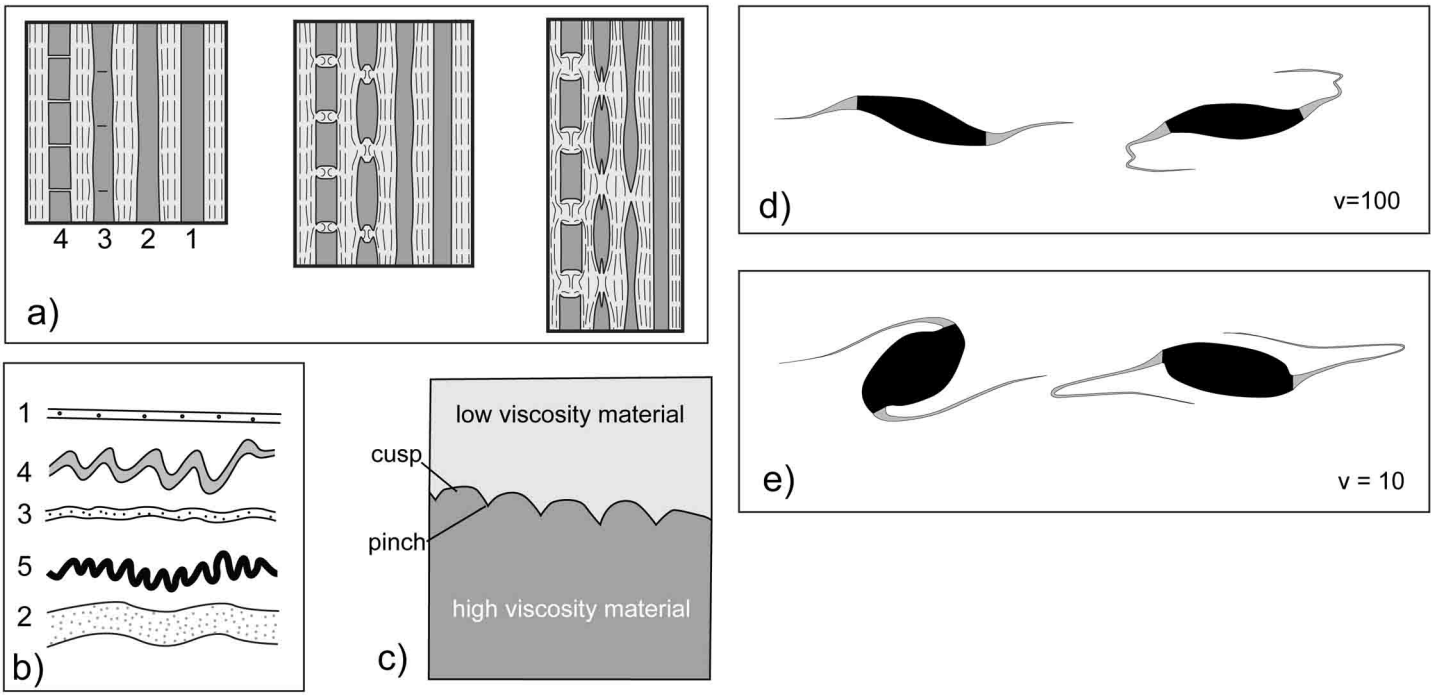

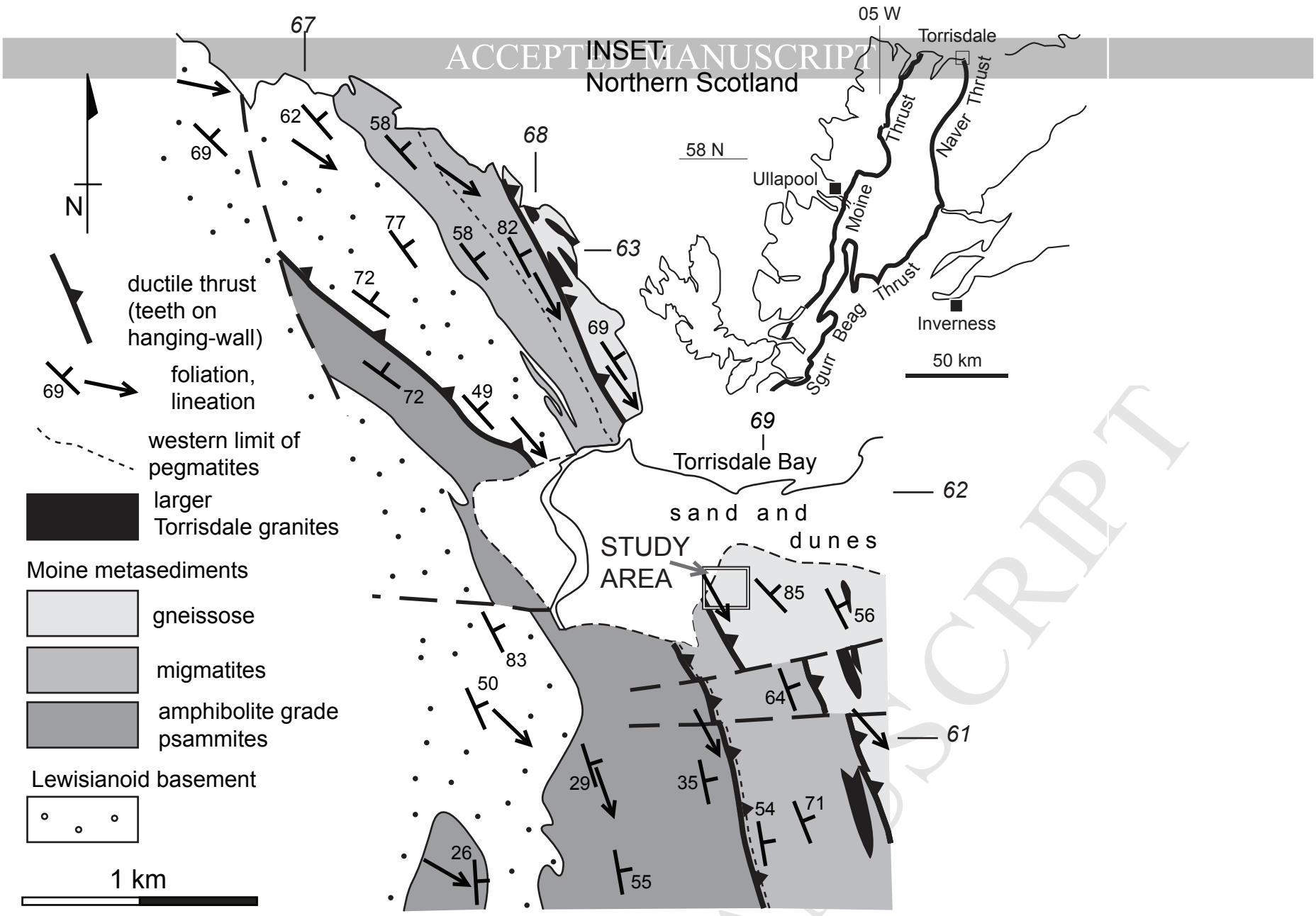

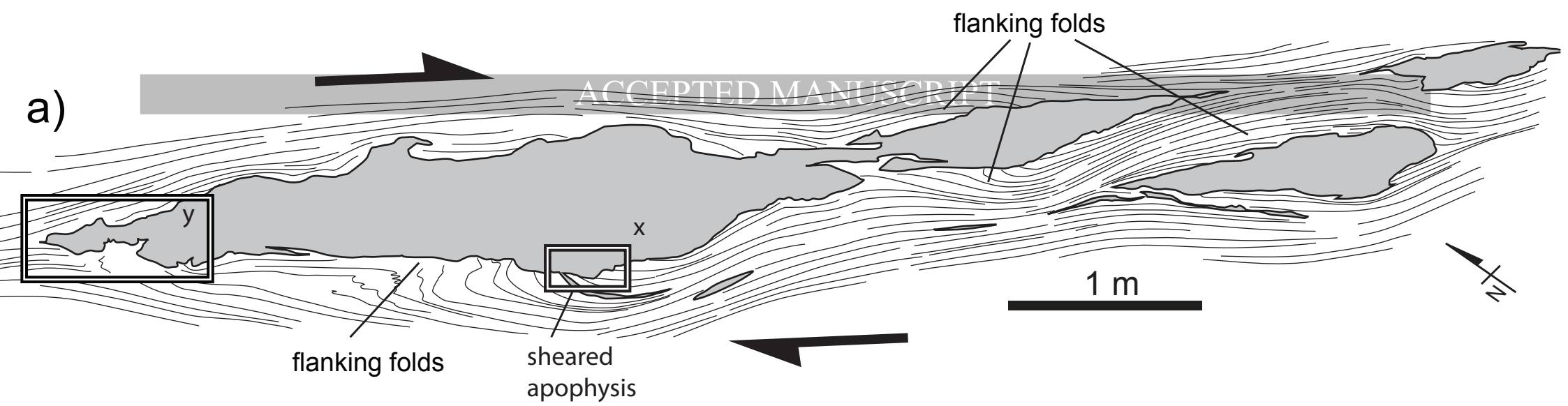

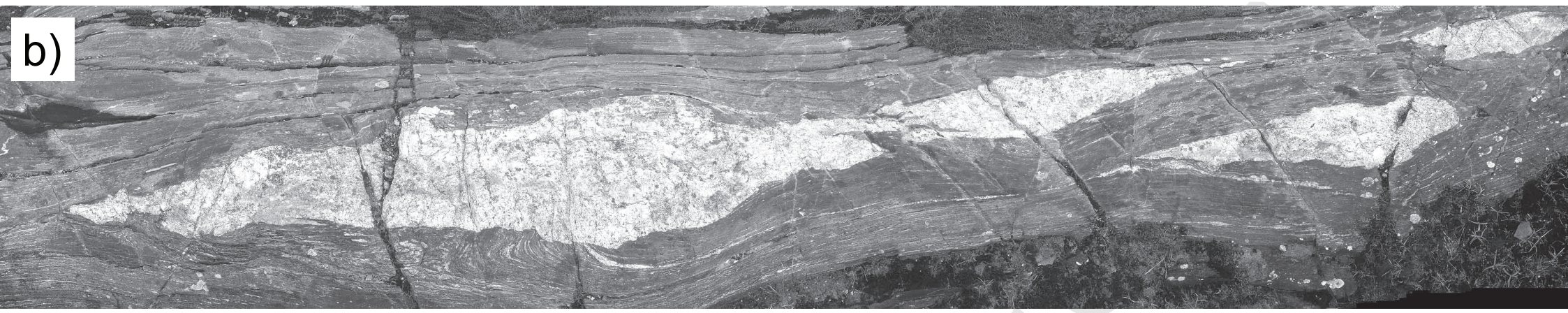

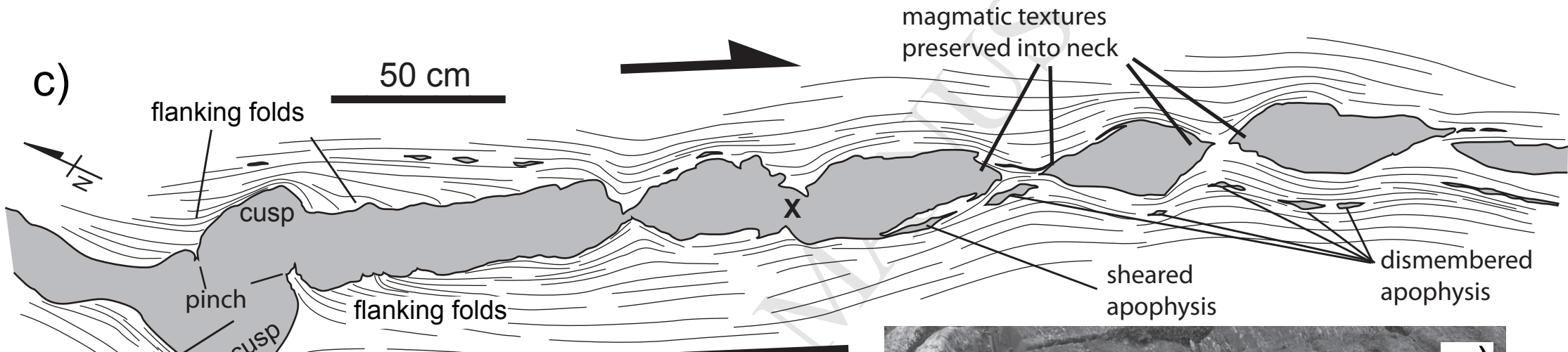

Figure 4 (part 2)

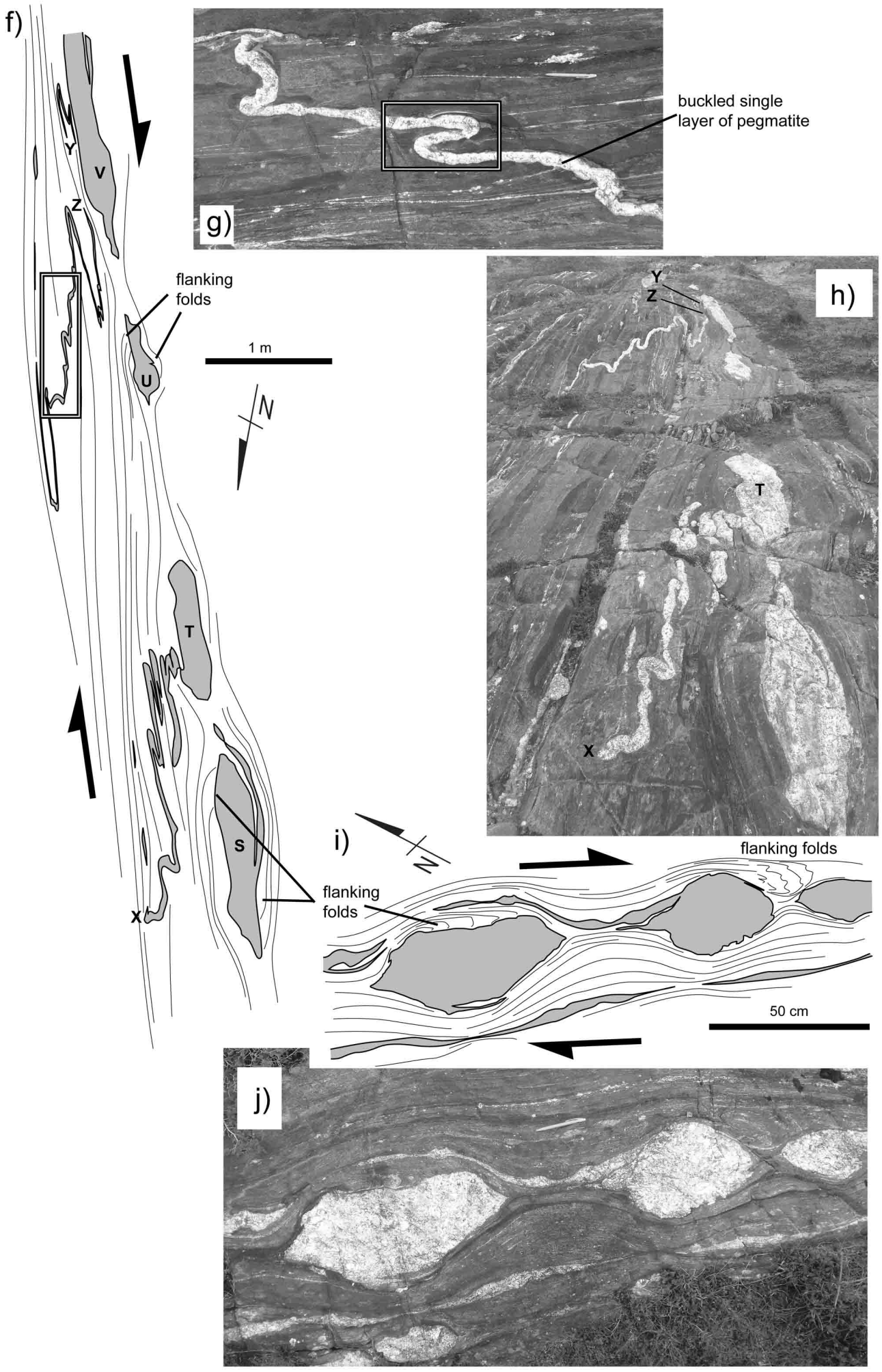

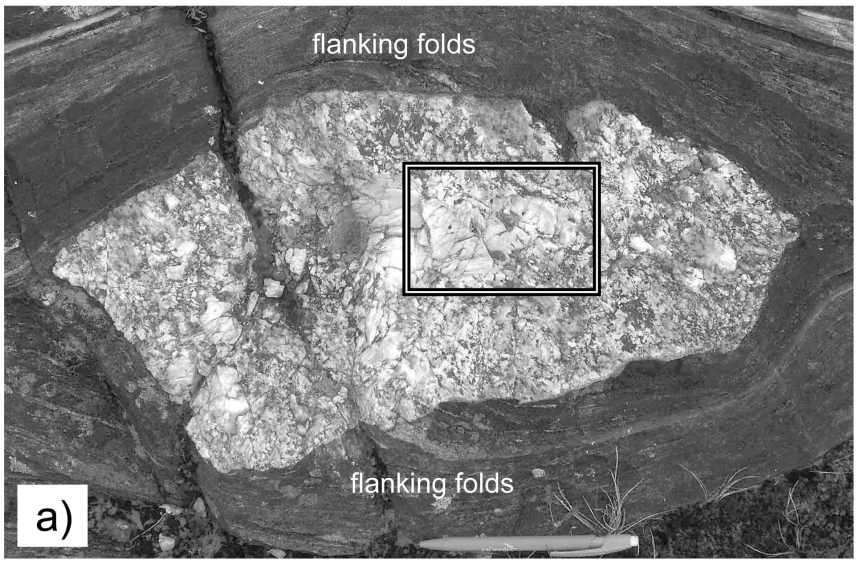
flanking folds
flanking folds
a)

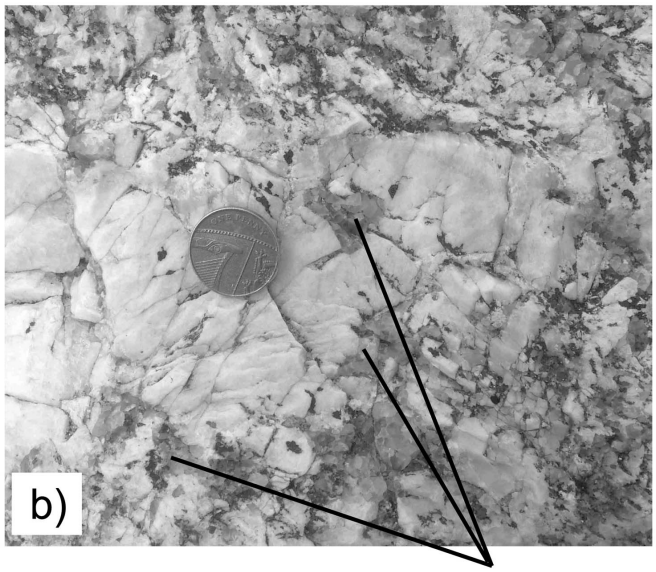
b)
domains of polycrystalline quartz

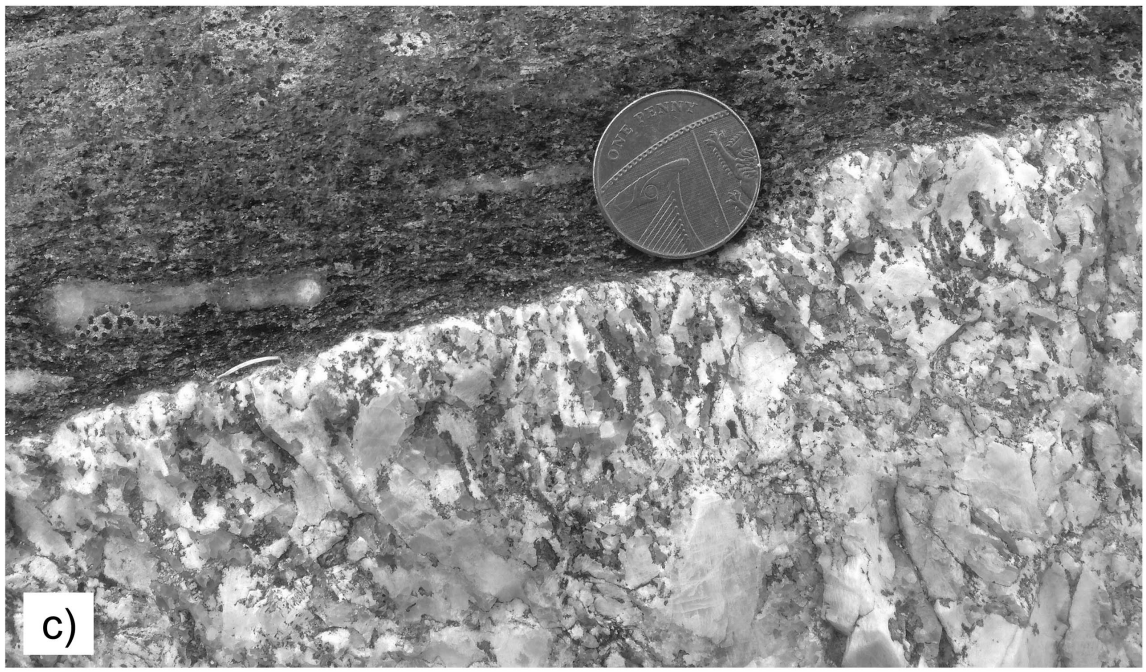
c)
marginal facies
coarse internal facies

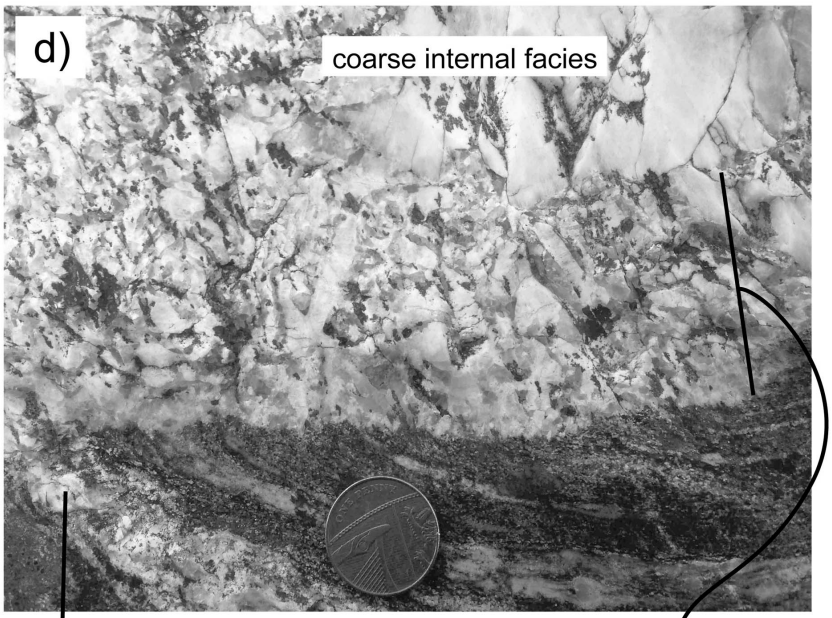
d)
coarse internal facies
sheared apophysis
marginal facies

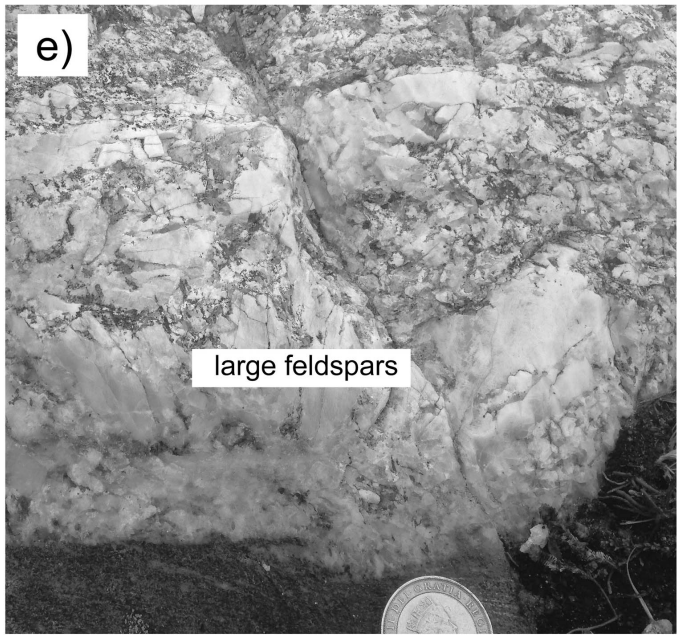
e)
large feldspars

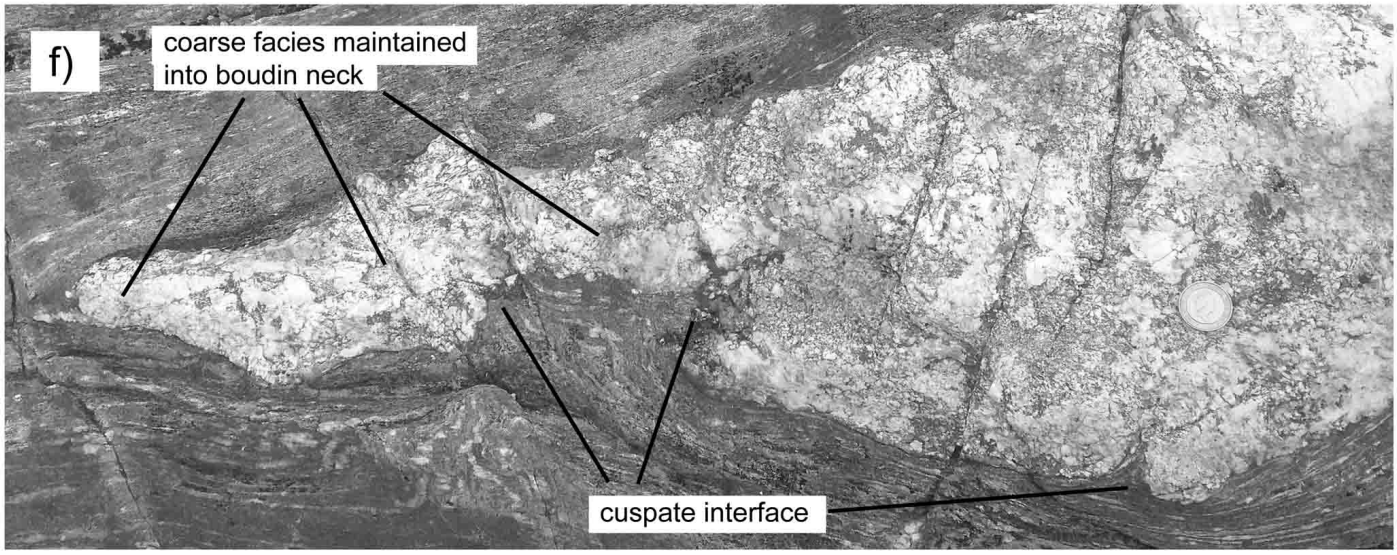

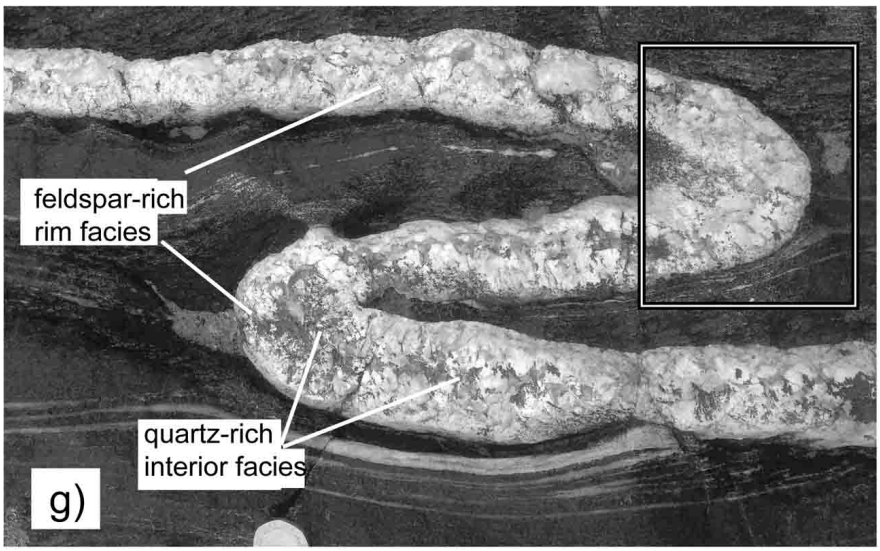

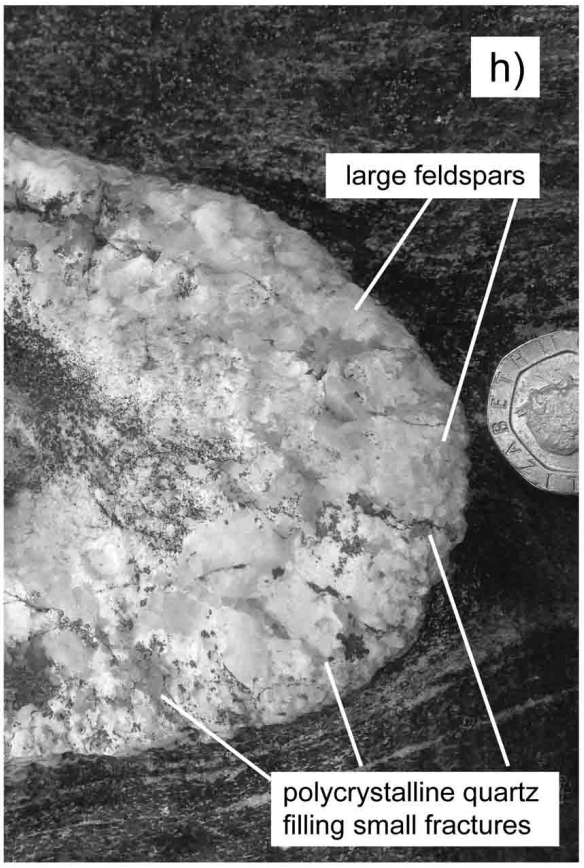

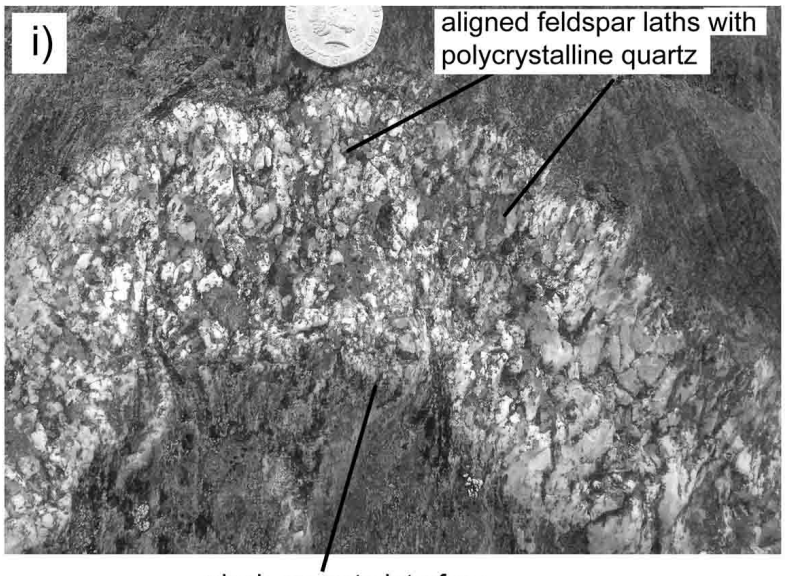

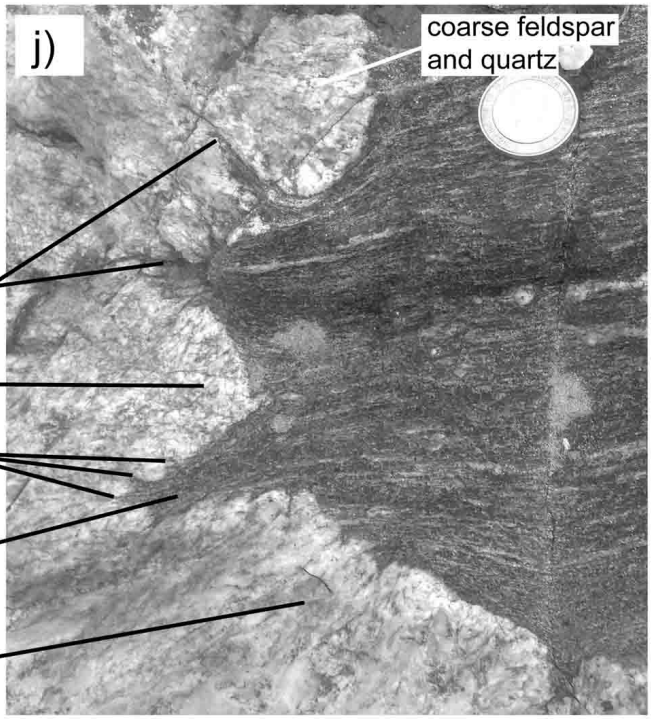

Figure 5 (part 2)

Figure 6

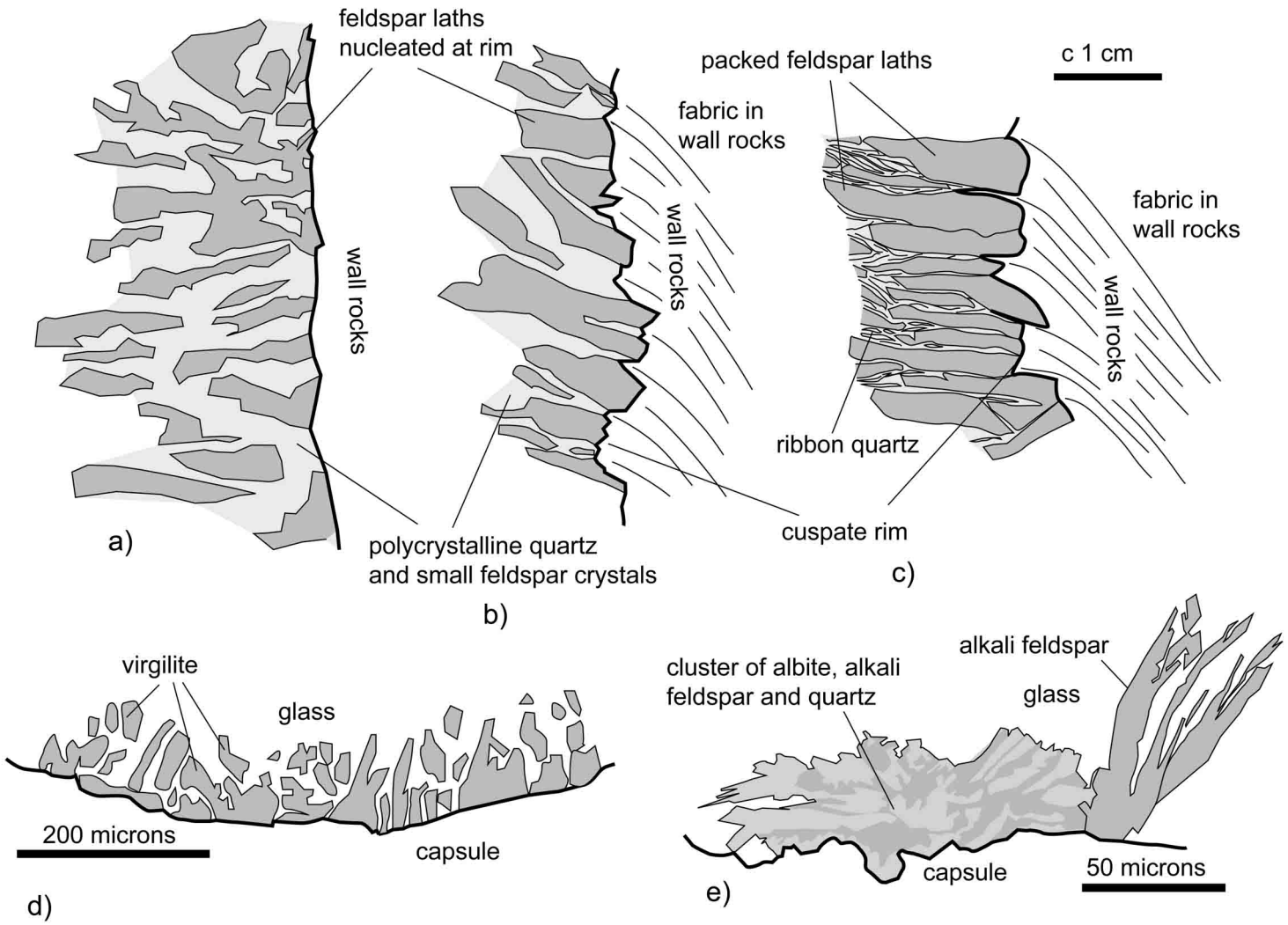
feldspar laths
nucleated at rim
wall rocks
a)
polycrystalline quartz
and small feldspar crystals
b)
fabric in
wall rocks
wall rocks
packed feldspar laths
c 1 cm
fabric in
wall rocks
wall rocks
ribbon quartz
cuspate rim
c)
virgilite
glass
200 microns
capsule
d)
alkali feldspar
cluster of albite, alkali
feldspar and quartz
glass
capsule
50 microns
e)

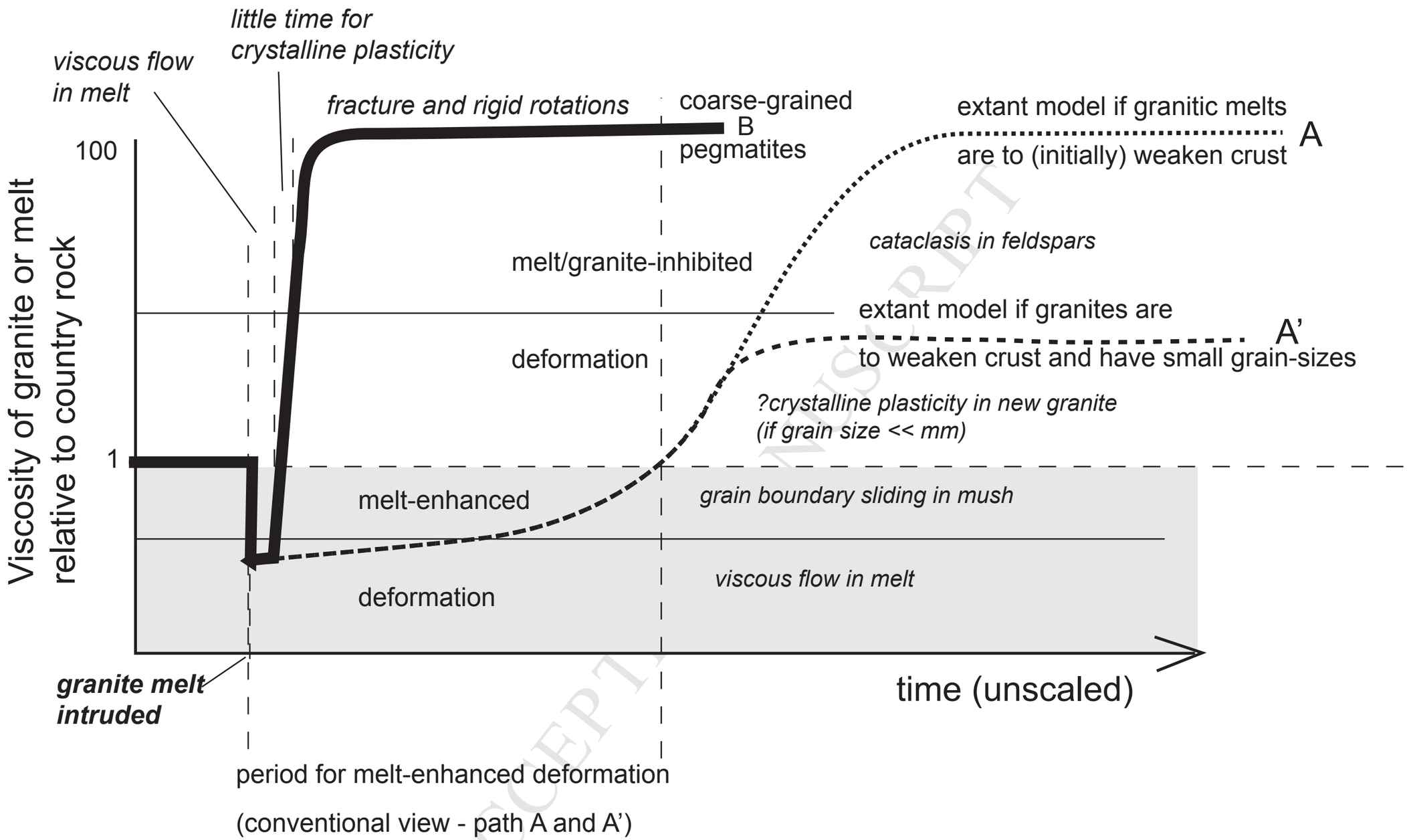

Highlights

- Typical field relationships in syn-tectonic pegmatites are re-evaluated.
- Pegmatites have igneous textures but deformed as strong, not weak inclusions.
- Initial crystallization forms coarse-grained stiff rinds that enclose residual melts.
- Experiments show that competent rinds can crystallize in less than a year.
- Deforming crust is strengthened, not weakened by injection of hydrous siliceous melt.